ELSEVIER

Polymer 41 (2000) 6755–6764

polymer

Ionic conductivity of polymer electrolytes derived from various diisocyanate-based waterborne polyurethanes

Ten-Chin Wen[a,*], Shih-Sheng Luo[a], Chien-Hsin Yang[b]

[a]*Department of Chemical Engineering, National Cheng Kung University, Tainan, 701, Taiwan, ROC*
[b]*Department of Environmental and Chemical Engineering, Kung Shan Institute of Technology, Tainan, Taiwan, ROC*

Received 4 June 1999; received in revised form 22 November 1999; accepted 6 December 1999

Abstract

Various diisocyanate-based waterborne polyurethanes (WPU) were synthesized by polyaddition of poly(propylene glycol) (PPG) and dimethylol propionic acid (DMPA) with various diisocyanates ((4,4′-methylenebis(phenyl isocyanate) (MDI), 4,4′-methylenebis(cyclohexyl isocyanate)(H_{12}MDI), isophorone diisocyanate (IPDI), and toluene diisocyanate(TDI)) via our modified acetone process. Differential scanning calorimetry (DSC), Fourier-transform infrared spectroscopy (FTIR), and impedance spectroscopy (IS) were utilized to monitor the phase change and the conductivity of the WPU-based electrolytes with the doped lithium perchlorate ($LiClO_4$) concentration. The soft segment T_g increases with increasing $LiClO_4$ from the examination of DSC. Significant changes occur in the FTIR spectrum of the various diisocyanate-based WPUs with adding $LiClO_4$, indicating that different interactions with the lithium cation within the hard segment and between the hard and soft phases occur. The result reflects that the phase separation of aromatic diisocyanate-based WPU is more significant than that of aliphatic one in the addition of salts. IS results indicate that there exists the different effect of the added lithium salt on conductivity for aromatic/aliphatic diisocyanate-based WPU electrolytes.

Keywords: Polymer electrolytes; Diisocyanate-based waterborne polyurethanes; Ionic conductivity

1. Introduction

Among the various polymer electrolytes developed, polyether-based electrolytes desired features such as good adherence to the electrode and ability to dissolve many inorganic salts forming a homogeneous solution. The dissolution of alkali-metal salts in polyether polymers has been extensively studied [1,2]. The dissociation is characterized by the formation of transient cross-links between ether oxygens in the host polymer and alkali-metal cations; the anions are usually not solvated. Ionic transport is achieved through a coupling between the ions and polymer segmental motion; hence, to obtain higher ionic conductivity ($>10^{-5}$ S/cm) which is useful in ambient-temperature applications such as solid state batteries [3] and fuel cells [4], polymer possessing high flexibility is required.

In our laboratory, a series of studies [5–8] have been performed for the polymer electrolytes on the basis of waterborne polyurethane (WPU). In particular, the system of polypropylene glycol/isophorone diisocyanate (PPG/IPDI) [9] has been studied through several spectroscopic examination. Significant changes occur in the FTIR spectrum of the WPU with the added salt ($LiClO_4$) concentration above 1 mmol/g WPU, indicating that an interaction with the lithium cation within the hard segment and between the hard and soft phase occurs. The soft segment T_g increases with increasing $LiClO_4$ through the examination of the differential scanning calorimetry (DSC) thermograms. XPS results reveal that the component of nitrogen polaron sites (N^+) increases with increasing $LiClO_4$ and the saturation level of salt doping is evidenced by the mole ratio of component C–O to C=O.

Polyurethanes (PUs) are composed of polyether or polyester soft segment and a diisocyanate-based hard segment, which can be characterized by a two-phase morphology [10]. The phase separation is due to the fact that the hard and soft phases are immiscible and leads to the formation of a hard-segment domain, a soft-segment matrix, and an ill-defined interphase. The hard-segment domains act as physical cross-links and filler particles to the soft segment matrix. The domain formation is derived from the intermolecular hydrogen bonding between the hard–hard segments of urethane or urea linkages. The hydrogen bonding is characterized by a frequency shift to the values lower than those corresponding to the free groups (i.e. no

* Corresponding author. Tel.: + 886-6-2757-575; fax: + 886-6-2344-496.
E-mail address: tcwen@mail.ncku.edu.tw (T.-C. Wen).

0032-3861/00/$ - see front matter
PII: S0032-3861(00)00023-9

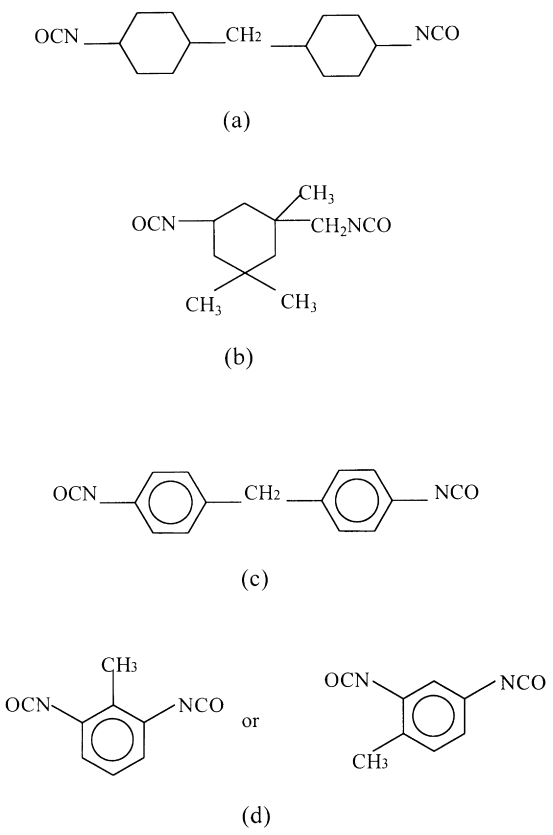

Fig. 1. The chemical structures of various diisocyanates: (a) H_{12}MDI; (b) IPDI; (c) MDI; (d) TDI.

hydrogen bonding) in the FTIR spectrum. Meanwhile, the extent of the frequency shift is usually used as an estimate of hydrogen-bonding strength. Particularly for polyether-based PUs, the fraction of the hydrogen-bonded carbonyls is defined by a hard–hard segment hydrogen bond (N–H···O=C bond), which was employed to evaluate the extent of phase separation. On the other hand, the fraction of the hydrogen-bonded ether oxygens (N–H···O–) represents the extent of phase mixing between hard and soft segments.

In this work, PPG-based WPU electrolytes were extended from the previous [9] to others by using various diisocyanates (4,4′-methylenebis(phenyl isocyanate) (MDI), 4,4′-methylenebis(cyclohexyl isocyanate) (H_{12}MDI), isophorone diisocyanate (IPDI), and toluene diisocyanate (TDI)) as hard segments. These WPUs were synthesized and used as polymer electrolytes. By using FTIR, DSC, and impedance spectroscopy (IS), we investigate the effect of various types of diisocyanates on phase variation, morphology characteristics and bulk conductivity of these WPU electrolytes.

2. Experimental

2.1. Synthesis of WPU dispersions

Four types of WPU dispersions were prepared through our modified acetone process [11,12] by polyaddition of various diisocyanates (4,4′-methylenebis(phenyl isocyanate) (MDI), 4,4′-methylenebis(cyclohexyl isocyanate) (H_{12}MDI), isophorone diisocyanate (IPDI), and toluene diisocyanate (TDI)) to poly(oxypropylene) glycol (PPG) and dimethylolpropionic acid (DMPA), followed by neutralization of pendant COOH with LiOH. The chemical structures of the diisocyanates employed in this study are shown in Fig. 1. PPG was dried and degassed under vacuum at 70°C for 2 days. DMPA was also dried under vacuum at 120°C and then dissolved in DMF which was distilled over anhydrous $MgSO_4$ at low pressure and stored over 3 Å molecular sieve before use. The preparation of chain extender was similar to that in our previous paper [11] except using LiOH instead of NaOH.

2.2. Preparation of polymer films

WPU dispersions were poured on a Teflon disk at ambient conditions. After pouring, we allowed sufficient time to elapse for most of the water, and the residual moisture was further removed by vacuum pumping at 60°C for 3 days.

The desired lithium salt-doped polymer film was prepared by dissolving the cast film in acetone with proper $LiClO_4$/acetone solution. The solution was then cast under vacuum for 3 days at 60°C to form 0, 0.5, 1, and 2 mmol $LiClO_4$/g WPU polymer films doped as samples a–d, respectively.

The films were then stored in an argon-filled dry box (Vacuum Atmosphere, USA). Before all tests of these films, the water content of these films was determined to be around 10 ppm by using Karl Fisher moisture titration meter (MKC-210, Kyoto Electronics, Japan).

2.3. DSC thermograms

Thermal analysis of WPU was carried out using DSC (TA 2010, USA) over the temperature range of −100 to +150°C at a heating rate of 10°C/min. Sample was taken from WPU film and sealed in aluminum capsules for analysis.

2.4. Infrared spectroscopy

Films for infrared analysis were prepared by casting 5% DMF solutions onto potassium bromide windows at room temperature. Following evaporation of the majority of the solvent, the films were placed in a vacuum oven at about 80°C for over 24 h to remove residual solvent and moisture. Similarly, the films were stored in an argon-filled dry box. Then, the samples were transferred to the holder in the spectrometer.

FTIR spectra were collected using a Nicolet 550 system at a resolution of 2 cm^{-1}, and a minimum of 64 scans were signal-averaged at room temperature. Band deconvolution of the resulting spectra was obtained by analysis with GRAMS 386 software (Galactic). The maximum error

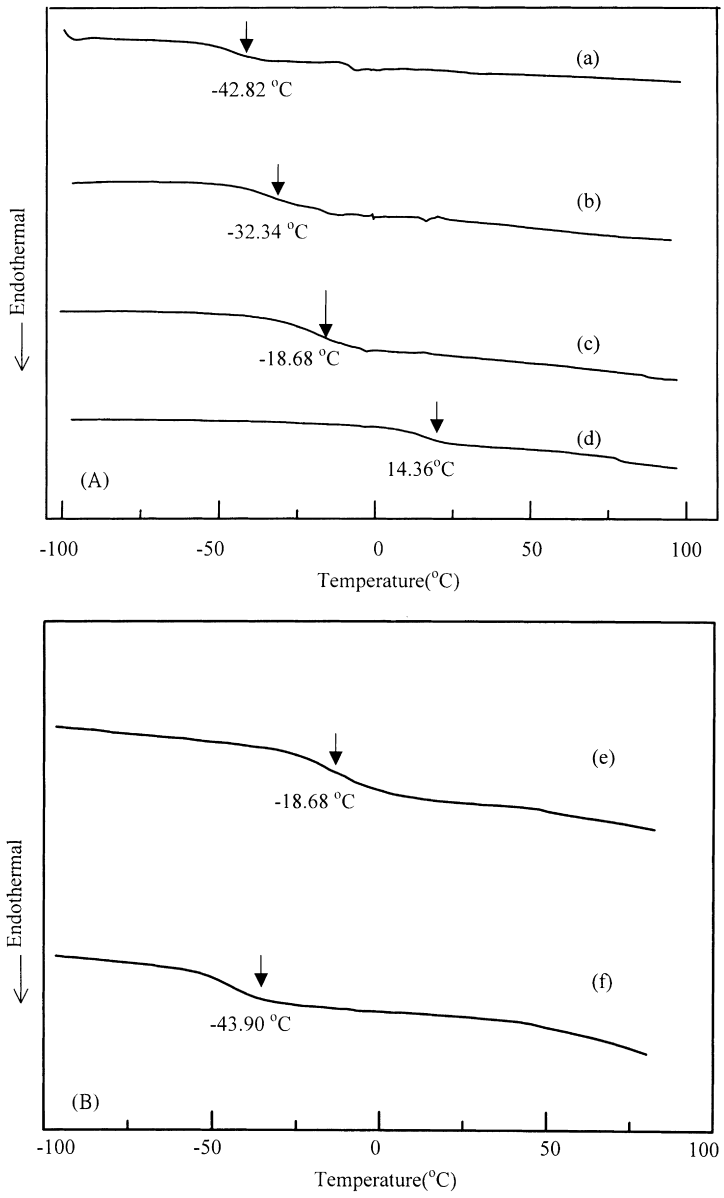

Fig. 2. (A) DSC thermograms for WPU (PPG/H_{12}MDI) electrolytes containing different $LiClO_4$ concentrations: (a) 0, (b) 0.5, (c) 1, (d) 2 mmol/g WPU. (B) DSC thermograms for WPU (PPG/H_{12}MDI) electrolytes containing $LiClO_4$ 1 mmol/g WPU: (e) no PC (f) 50% PC.

associated with the deconvolution of the IR spectra is expected to be ±5%. In most cases, the deconvolution was executed by fitting the spectra to different functions to assure the accuracy of the deconvolution results.

2.5. Impedance spectroscopy

Impedance measurements were performed using thin films prepared previously of about 150 μm in thickness and 0.785 cm^2 in area. The ionic conductivity of the WPU films sandwiched between two stainless steel electrodes was obtained by using CMS300 EIS (Gamry Instruments, Inc., USA) together with an SR810 DSP lock-in amplifier (Stanford Research Systems, Inc., USA) under an oscillation potential of 10 mV from 100 kHz to 0.1 Hz.

3. Results and discussion

3.1. Differential scanning calorimetry

DSC was used to examine the effect of $LiClO_4$ on the polyether soft-segment T_g of these WPUs. Fig. 2A shows that T_g of the PPG soft-segment for the PPG/H_{12}MDI system increases with increasing salt concentration. Similar results exist in other system of different diisocyanates (e.g. PPG/IPDI, PPG/MDI, and PPG/TDI). This is consistent with our previous work [9] and other investigations of TPUs containing either PEO [13,14] or PPO [15,16] as the soft segment. This indicates that the solvation of the lithium cation by the PPO soft-segment partially arrests the local motion of the polymer segment through the formation of

Table 1
Glass transition temperature (T_g) for $LiClO_4$-doped WPUs

$LiClO_4$ (mmol/g WPU)	PPG/MDI		PPG/H_{12}MDI		PPG/IPDI		PPG/TDI	
	T_g (°C)	$\Delta T_g/\Delta c$ (°C/mmol/g WPU)	T_g (°C)	$\Delta T_g/\Delta c$ (°C/mmol/g WPU)	T_g (°C)	$\Delta T_g/\Delta c$ (°C/mmol/g WPU)	T_g (°C)	$\Delta T_g/\Delta c$ (°C/mmol/g WPU)
0.0	−26.47		−42.82		−38.34		−34.06	
0.5	−10.81	31.32	−32.34	20.96	−26.85	22.98	−21.3	25.52
1.0	−2.73	16.16	−18.68	27.32	−16.83	20.4	−13.06	16.48
2.0	11.81	14.54	14.36	33.04	−3.77	13.06	2.86	15.92

transient cross-links, leading to an increase in the soft-segment T_g. By normalizing the T_g data against salt concentration for these WPU films, the value of $\Delta T_g/\Delta c$ was calculated at each measurement and which are listed in Table 1. It is obvious that a non-linear increase in T_g is observed with increasing salt concentration. The value of $\Delta T_g/\Delta c$ decreased with increasing salt concentrations except for the PPG/H_{12}MDI system. This result is attributable to the plasticizing effect generated by the formation of charge–neutral contact ion pair with increasing salt concentration [17]. The neutral contact ion pairs lose the ability to provide ionic cross-links; hence, the further increase in T_g is insignificant. It is worthwhile to note that the $\Delta T_g/\Delta c$ of PPG/H_{12}MDI system is increased upon increasing salt concentration. This result reflects that the salt doping level for PPG/H_{12}MDI WPU has not been saturated in the range of 0–2 mmol $LiClO_4$/g WPU. Thus, the lithium salt can be further dissolved and solvated with the oxygen on the soft-segment ether linkage.

The DSC results for the sample of $LiClO_4$/WPU complex with 50% PC is shown in Fig. 2B. It is obvious that the T_g of PPG soft-segment in the PPG/H_{12}MDI WPU is decreased from −18.68 to −43.90°C by the intake of 50% PC. This indicates that the solvated degree of the lithium cation with the oxygen of soft-segment ether linkage is decreased. Consequently, T_g is decreased due to the enhanced mobility of the soft-segment by PC solvent. Similar results existed in other system of different diisocyanates. This result is related to a significant increase in electrical conductivity when PC is added into the $LiClO_4$/WPU complex (see Figs. 6 and 7).

3.2. Infrared analysis

FTIR was utilized at ambient temperature (25°C) to study the effect of salt concentration on the phase morphology of these WPUs. Two major spectrum regions are of the main interest: the N–H stretching vibration (3000–3650 cm^{-1}) and the carbonyl stretching vibration (1690–1800 cm^{-1}).

3.2.1. N–H stretching region

Fig. 3 shows the typical IR spectrum of the N–H stretching region of PPG/H_{12}MDI-based WPU film. In this spectrum, the N–H stretching vibration exhibits a strong absorption peak at around 3330 cm^{-1} (peak II) arising from the hydrogen bonding between N–H and carbonyl groups, whereas the free N–H stretching vibration appears at ca. 3500 cm^{-1} (peak I). Note that there exists another

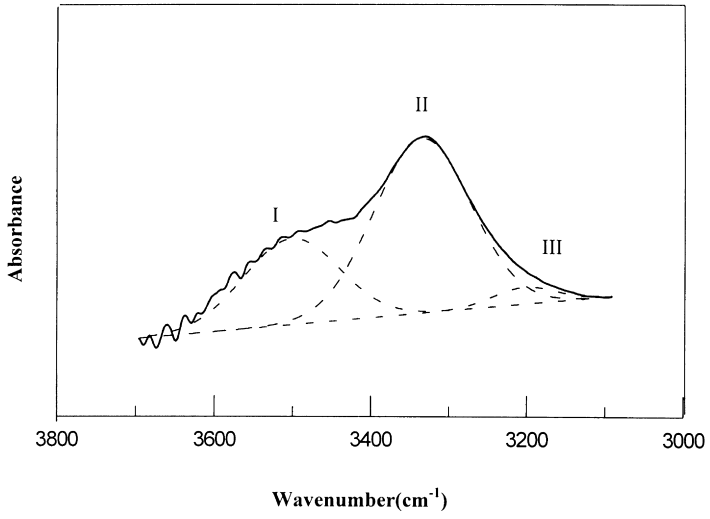

Fig. 3. The FTIR spectrum (solid line) and decomposition curves (dashed lines) of WPU electrolytes (PPG/H_{12}MDI) in the N–H stretching region.

Table 2
Decomposition results of various WPUs in the N–H stretching region

Film	$LiClO_4$ (mmol/g WPU)	Peak position (cm^{-1})			Peak area[a] (%)		
		I	II	III	I	II	III
PPG/H_{12}MDI	0.0	3509	3334	3203	35.20	60.88	3.92
	0.5	3510	3336	3234	49.18	41.97	8.84
	1.0	3516	3365	3244	42.43	40.61	16.97
	2.0	3530	3381	3253	36.96	40.35	22.69
PPG/IPDI	0.0	3510	3334	3174	34.50	63.26	2.24
	0.5	3533	3395	3276	31.75	42.75	25.51
	1.0	3550	3420	3298	26.22	40.29	33.49
	2.0	3591	3487	3307	23.90	32.99	43.12
PPG/MDI	0.0	3478	3302	3188	34.48	63.14	2.39
	0.5	3479	3302	3188	50.84	44.77	4.38
	1.0	3577	3419	3242	28.65	39.23	32.12
	2.0	3578	3463	3294	12.37	40.02	47.60
PPG/TDI	0.0	3496	3306	3178	38.08	60.02	1.91
	0.5	3497	3318	3179	50.45	46.02	3.53
	1.0	3559	3444	3295	18.78	43.28	37.94
	2.0	3576	3468	3307	16.44	34.87	48.69

[a] The band areas are based on the total N–H stretching area.

shoulder at ca. 3200 cm^{-1} (peak III). This peak corresponds to the NH···O– hydrogen bonding [18]. This result is attributable to the phase-mixed state between hard and soft-segment via hydrogen bonding in the polymers.

Deconvolution of the N–H stretching region was found to be the best fits by using a Gaussian–Loretzian sum. The maximum frequency (ν) and area of each band were determined by using the Nelder–Mead optimization method. All N–H band areas were normalized on the basis of total N–H stretching band area and are listed in Table 2. The band shift of three decomposition peaks is approximately proportional to the salt concentration. The peak position of free N–H stretching (peak I) with external doping salt is higher than that peak position (3440 cm^{-1}) without the doping salt. This situation is presumably due to the interaction between the Li^+ cation and the lone pair of electrons on nitrogen atom [19], leading to the reduction of N–H bond length as seen in Fig. 4(a). Thus, the vibration energy of N–H bond is relatively increased when the external salt is doped in WPU film, resulting in a higher frequency of absorption peak. An examination of Table 2 shows that the area ratio of peak I is insignificantly influenced by the concentration of doping salt for PPG/H_{12}MDI and PPG/IPDI systems. On the other hand, the area ratio of peak I significantly depends upon the concentration of doping salt for PPG/MDI and PPG/TDI systems. These results reflect that the effect of the added lithium salt on the free N–H stretching region is different for both of aliphatic and aromatic hard segments.

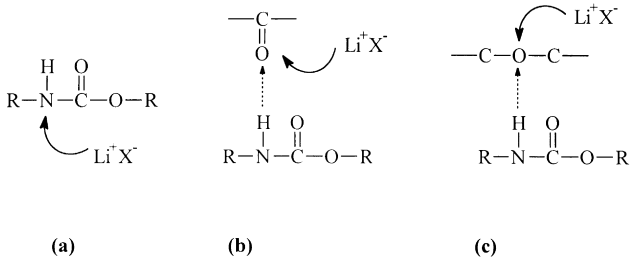

Fig. 4. Schematics for the suggested coordination of the lithium cation with the PPG-based WPU.

In Table 2, the component of peak II corresponds to hydrogen bonding between N–H and carbonyl groups [20]. The position of this component shifts to higher frequency as the salt concentration increases for all of these WPUs. Because band position is related to the strength of H-bonded N–H bond, the shift to higher frequency with increasing salt concentration indicates a decrease in the H-bonded strength. Therefore, the H-bonding strength is decreased with increasing salt concentration. This is possibly due to the localization of the electron-rich oxygens on the carbonyl through coordination of the Li^+ cation with the H-bonded species, as shown in Fig. 4(b). Furthermore, the band area (peak II) decreased with increasing salt concentration in Table 2. This result reflects that the possibility of the hydrogen bonding between N–H and carbonyls is decreased.

Note that Table 2 reveals the band position of hydrogen bonding of N–H to –O– (ether oxygens) (peak III) [20] of PPG soft segment is also shifted to higher frequency with the addition of salt. This shift of frequency to higher values increases with increasing salt concentration, implying that the more added lithium salt in WPU gives the stronger band strength of the N–H bond. This is likely due to the coordination of non-bonded electrons on the ether oxygens with the Li^+ cation, leading to a weakening of

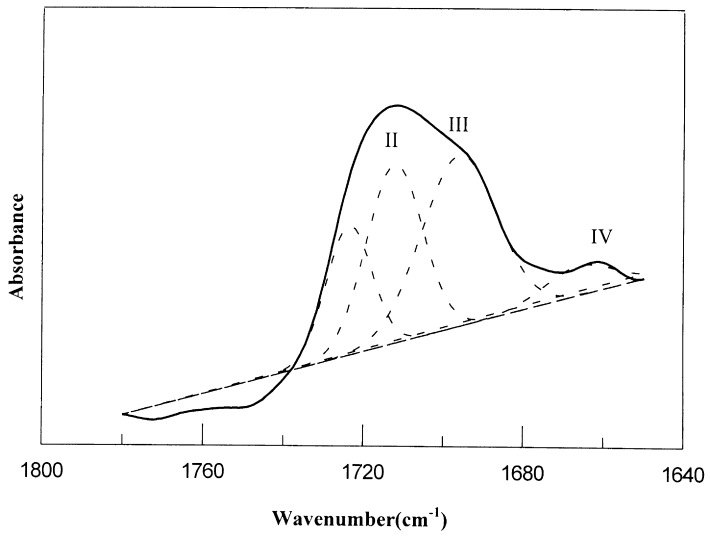

Fig. 5. The FTIR spectrum (solid line) and decomposition curves (dashed lines) of WPU electrolytes (PPG/H_{12}MDI) in the carbonyl stretching region.

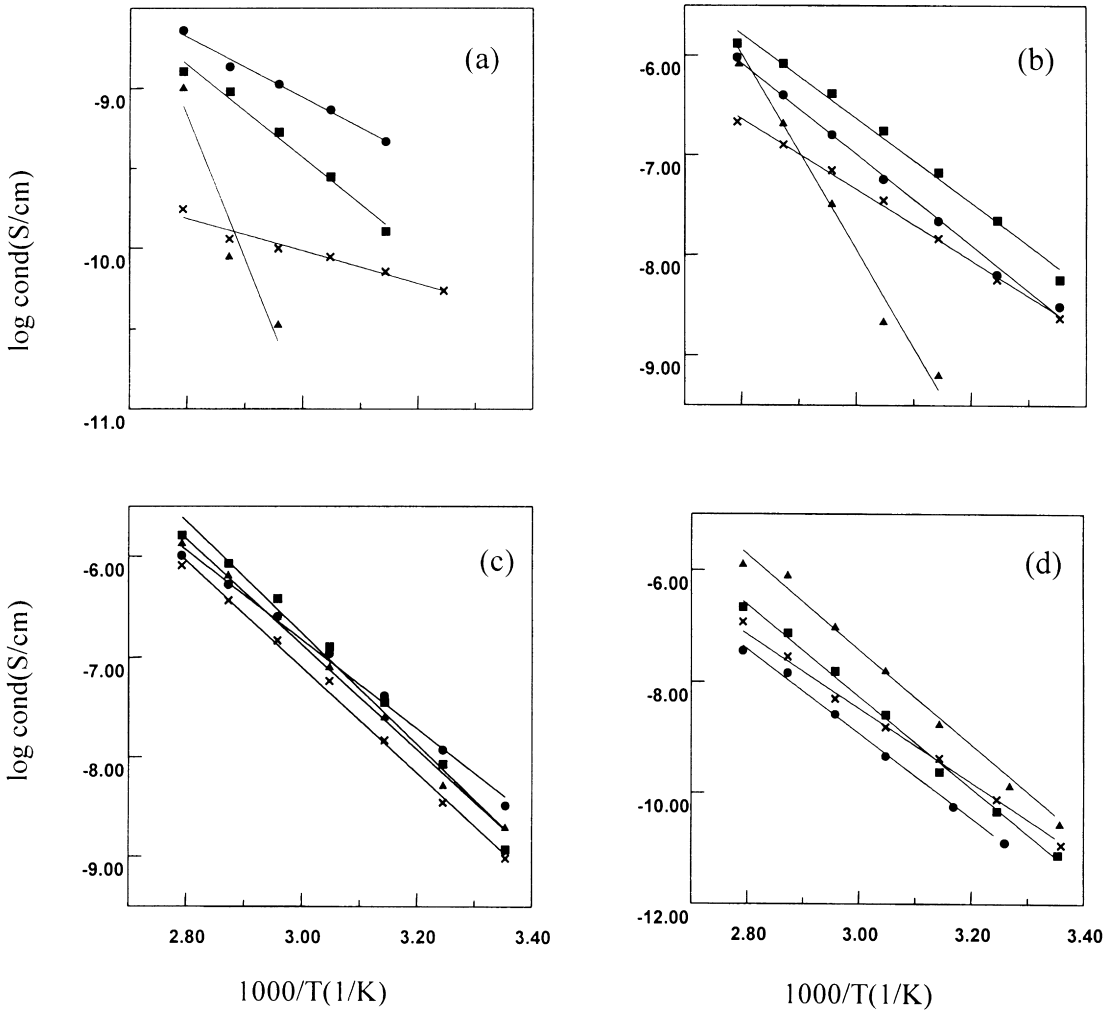

Fig. 6. The dependence of conductivity on the reciprocal of temperature for different PPG/isocynate based WPUs containing various $LiClO_4$ concentrations (in mmol/g WPU): (a) 0; (b) 0.5; (c) 1; (d) 2. Symbols: (▲) PPG/MDI-based WPU; (●) PPG/H_{12}MDI-based WPU; (×) PPG/IPDI-based WPU; (■) PPG/TDI-based WPU.

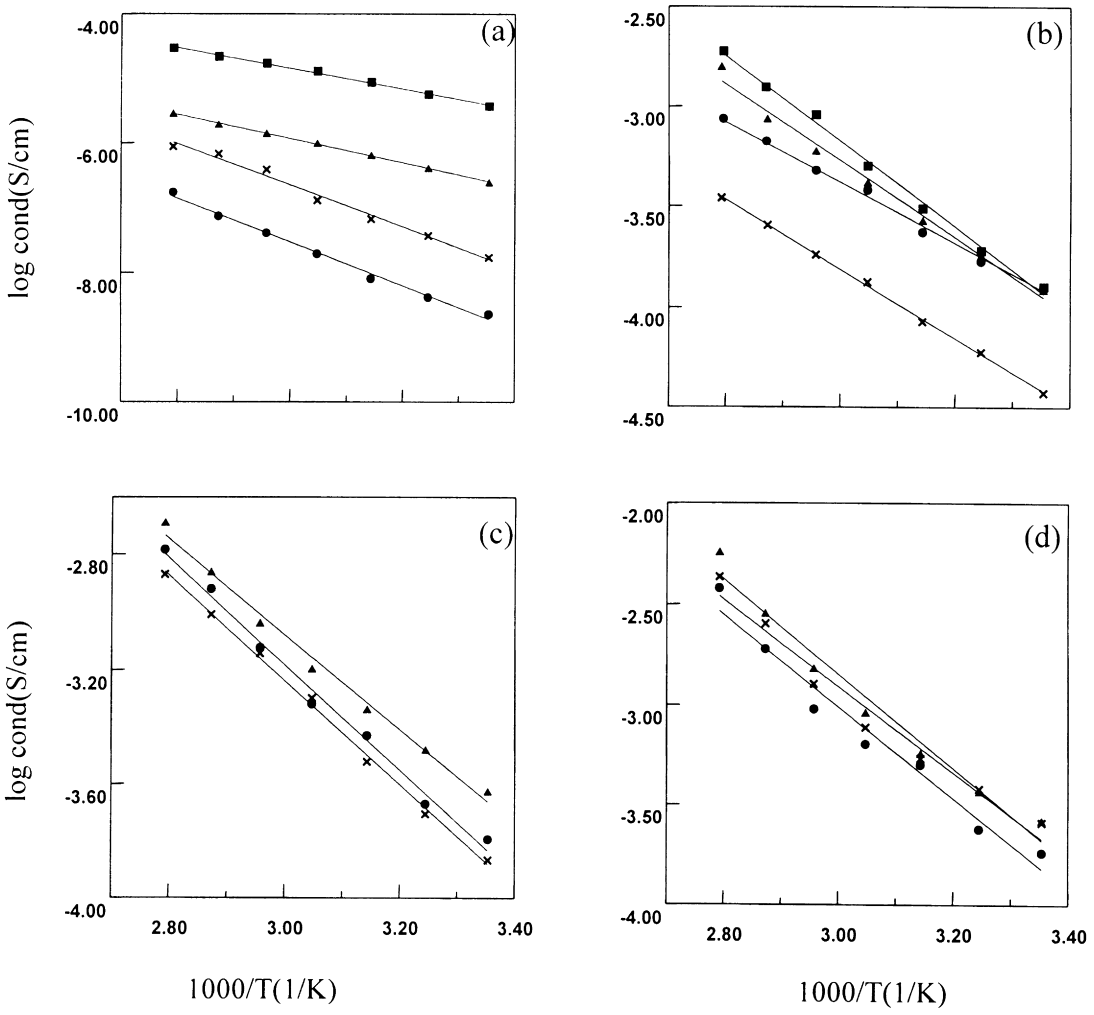

Fig. 7. Arrhenius plots of conductivity for different PPG/diisocynate-based WPUs containing various $LiClO_4$ concentrations (mmol/g WPU) in 50% PC: (a) 0; (b) 0.5; (c) 1; (d) 2. Symbols: (▲) PPG/MDI-based WPU; (●) PPG/H_{12}MDI-based WPU; (×) PPG/IPDI-based WPU; (■) PPG/TDI-based WPU.

the hydrogen-bonded strength between N–H and ether oxygens (see the model of Fig. 4(c)). An examination of Table 2 reveals that the band area of NH–ether (peak III) increases with increasing salt concentration. This can be attributed to the fact that the coordination of non-bonded electrons on ether oxygens with cation is increased, inducing an increase in hydrogen bonding between N–H and ether groups. This similar observation has been evidenced by XPS results [9].

3.2.2. C=O stretching region

Fig. 5 shows the IR spectrum of the carbonyl stretching region ranging from 1600 to 1750 cm^{-1} for PPG/H_{12}MDI-based WPU. The band centered at around 1724 cm^{-1} (peak I) is attributed to the stretching of free urethane carbonyl groups, whereas the band at 1712 cm^{-1} (peak II) is assigned to H-bonded urethane carbonyl groups. According to the previous study [21,22], the urethane carbonyl stretch at around 1710 cm^{-1} is due to hydrogen bonding in disordered regions, corresponding to carbonyl participating in urethane linkage of interfacial regions or being dissolved in the soft phase. For the stronger hydrogen bonds in ordered or crystalline regions, the stretching absorbance occurs at a lower frequency at ca. 1696 cm^{-1} (peak III). The band centered at ca. 1665 cm^{-1} (peak IV) is assigned to the stretching of H-bonded carboxylic carbonyl group, which comes from DMPA unit.

The deconvolution of the carbonyl region by Gaussian function was also performed and is listed in Table 3. For PPG/H_{12}MDI and PPG/IPDI WPUs, it is interesting that the stretching of free urethane carbonyl (peak I) shifts from higher to lower frequency when salt concentration is increased. This shift to a lower frequency suggests that the ionic coordination between the free urethane carbonyl and Li^+ cation increases with increasing salt concentration. For PPG/MDI and PPG/TDI WPUs, the stretching of free urethane carbonyl (peak I) first shifts to higher frequency with salt concentration of 0.5 mmol/g WPU, and then shifts back to lower frequency (in relative with salt concentration of 0.5 mmol/g WPU) when the salt concentration is further

Table 3
Decomposition results of various WPUs in the C=O stretching region

Film	$LiClO_4$ (mmol/g WPU)	Peak position (cm^{-1})			Peak area[a] (%)		
		I	II	III	I	II	III
PPG/H_{12}MDI	0.0	1724	1712	1696	30.49	34.84	34.67
	0.5	1723	1713	1696	26.95	36.83	36.22
	1.0	1721	1709	1694	26.55	29.91	43.54
	2.0	1720	1710	1693	13.09	27.48	59.43
PPG/IPDI	0.0	1724	1711	1693	24.71	44.98	30.31
	0.5	1724	1711	1694	22.00	42.33	35.67
	1.0	1723	1711	1695	21.70	34.86	43.44
	2.0	1722	1711	1696	17.17	34.23	48.60
PPG/MDI	0.0	1729	1709	1690	51.98	38.65	9.37
	0.5	1736	1726	1710	19.87	31.21	48.91
	1.0	1734	1727	1712	19.54	28.64	51.83
	2.0	1730	1725	1708	16.37	27.83	55.80
PPG/TDI	0.0	1728	1709	1693	61.31	20.74	17.94
	0.5	1736	1724	1707	23.71	33.12	43.17
	1.0	1735	1725	1710	18.93	36.24	44.83
	2.0	1734	1726	1710	16.08	33.40	50.53

[a] The band areas are based on the total carbonyl stretching area.

increased. These phenomena are related to the characteristics of aromatic groups in the hard segment.

The areas of the free urethane carbonyl groups (peak I) decrease with increasing salt concentration for all four types of WPUs. This is attributable to the fact that the ionic coordination between free urethane carbonyl and Li^+ increases with increasing salt concentration, leading to a decrease in the amount of free urethane carbonyl.

The stretching vibration band of disordered hydrogen bonded urethane carbonyl (peak II) occurs at $1711 \pm 2\ cm^{-1}$ for PPG/H_{12}MDI and PPG/IPDI WPUs, nearly independent of salt concentration. But this band position of PPG/MDI and PPG/TDI WPUs shifts to higher frequency, ca. $15\ cm^{-1}$ when salts are added. The difference between aliphatic and aromatic systems will be discussed along with the explanation for band area. The area of the disordered H-bonded urethane carbonyl decreases with increasing salt concentration. From DSC results, an increase in soft-segment T_g with increasing salt concentration indicates that the solvation of the lithium cation by PPG soft-segment partially arrests the local motion of the polymer segments through transient cross-links. Thereby, the amount of disordered H-bonded urethane carbonyl which participates in urethane linkage of interfacial regions or is dissolved in the soft phase will be reduced. This result reflects that the phase separation of aromatic WPUs is more significant than that of aliphatic samples in the addition of salts. The above explanation supports the results of band shift ca. $15\ cm^{-1}$ to higher frequency upon the addition of salt for aromatic samples.

The band position of ordered H-bonded urethane carbonyl (peak III) is nearly constant ($1695 \pm 2\ cm^{-1}$) for PPG/H_{12}MDI and PPG/IPDI WPUs. This band position of PPG/MDI and PPG/TDI WPUs shifts by about $2\ cm^{-1}$ to higher frequency when salt is added. Meanwhile, the area of the ordered H-bonded urethane carbonyl increases with increasing salt concentration for all four types of WPUs. The decrease in the amount of disordered H-bonded urethane carbonyl (peak II) will partially be transformed into ordered H-bonded urethane carbonyl (peak III) through the rearrangement of urethane orientation. It causes an increase in the ordered H-bonded urethane carbonyl with increasing salt concentration.

3.3. Ionic conductivity analysis

Since the four types of WPUs possess different characteristics from the above discussion, it is interesting to investigate the ionic conducting behavior of these samples. Thus, AC impedance was performed to determine the conductivity (σ) of these films. Fig. 6 illustrates the temperature dependence of ionic conductivity for the $LiClO_4$/WPU complex. The data without doping $LiClO_4$ salt are shown in Fig. 6(a), revealing that four straight lines with different slopes are obtained for four different types of WPUs. These results suggest that the Arrhenius phenomenological relationship

$$\sigma = A \exp[-E_a/RT] \quad (1)$$

can be used to describe the conductivity behavior for all four WPUs without doping salt. The Arrhenius form is employed when the ions are decoupled from the polymer host and activated hopping is required for ionic transport. At lower temperature, the magnitude of conductivity is in the order: GPPG/H_{12}MDI > PPG/IPDI > PPG/TDI > PPG/MDI. The strength of intermolecular H-bonding in PPG/MDI WPU is

the highest between these WPUs, which leads to the most significant phase separation. Because the Li^+ cation on the DMPA pendant group in this polymer chain is difficult to move, the ionic conductivity of PPG/MDI WPU is low. In contrast, the lithium ion on DMPA group in PPG/H_{12}MDI WPU is easy to move due to no aromatic bondage, resulting in a high conductivity.

At higher temperature, the strength of intermolecular/intramolecular H-bonding is reduced as the mobility energy of molecules increases. Therefore, the conductivity of four WPU samples are similar. In addition, the magnitude of the slope for four WPU samples is in the order: GPPG/MDI > PPG/TDI > PPG/H_{12}MDI > PPG/IPDI. This result implies that the temperature dependence of PPG/MDI WPU electrolytes without external doping salt is more sensitive than those of other WPUs.

In Fig. 6(b), the conductivity arises from the transport of lithium cation in the soft segment of WPU. This situation can be described by the Vogel–Tamman–Fulcher (VTF) equation

$$\sigma = AT^{1/2} \exp[-E_a/R(T - T_0)] \quad (2)$$

The application of the VTF form to ion transport in polymer electrolytes requires a coupling of mobile charge carriers to the segmental motion of the polymer host [23]. The most significant phase separation occurs in PPG/MDI WPU, the hydrogen bonding is slightly decreased at the salt doping level of 0.5 mmol/g WPU. Thereby, the slope for PPG/MDI WPU in Fig. 6(b) is similar to that in Fig. 6(a) when the concentration of lithium salt increased (1 mmol/g WPU), the hydrogen bonding is significantly decreased as reflected by the closeness of conductivity values and slope in Fig. 6(c). At a doping level of 2 mmol/g WPU (Fig. 6(d)), the conductivity is lower than that in Fig. 6(c) (1 mmol/g WPU salt doping).

The result of high salt doping level can be explained as follows: (i) the formation of ion pair increases with alkali-metal salt concentration [24], which limits the mobility of charge carriers in the polymer matrix; (ii) a considerable amount of salt is interacting or coordinating with the hard domain.

From the above results and discussion, the conductivity behavior of WPU doping with lithium salt can be summarized as follows:

1. For WPU without doping salt, there only exists small amount of lithium ions on the DMPA unit in the polymer chain. Thus, a high driving force is necessary for ionic conduction to be observed. This conductivity behavior obeys the Arrhenius equation.
2. As the doping salt has not yet reached to saturation level, the ions are predominantly coupled to the segmental motions of the host polymer. The ion transport in polymer electrolytes is improved with segmental motions of the polymer host. This conductivity behavior obeys the VTF equation.
3. As the lithium salt-doped level is saturated, the salt is incompletely able to participate in the conductive process. The formation of neutral ion pair increases with increasing salt concentration, which limits the mobility of charge carriers in the polymer matrix. This conductivity behavior also obeys the Arrhenius equation.

In order to understand the characteristics of WPU gel-type electrolytes, we added 50% propylene carbonate (PC) as a plasticizer into the above-mentioned WPU samples and then measured the temperature dependence of conductivity. The ions are decoupled from the polymer host and activated hopping is required for ionic transport after PC addition. Thus, the Arrhenius equation is used to describe this conductivity behavior. Fig. 7 shows the Arrhenius plot of ionic conductivity for the $LiClO_4$/WPU complex with the addition of 50% PC.

The temperature dependence of conductivity for WPU samples with 50% PC and without external doping salt is shown in Fig. 7(a). The conductivity is significantly increased with the addition of PC in WPU. This result suggests that the intermolecular H-bonding is decreased in these WPU samples, leading to a larger transport space of charge carriers (lithium ions). This explanation is consistent with the DSC results in which T_g of the PPG soft-segment is significantly decreased with the addition of PC. The magnitude of conductivity is in the order: PPG/TDI > PPG/MDI > PPG/IPDI > PPG/H_{12}MDI. In both aromatic WPUs of PPG/MDI and PPG/TDI, there exist more lone-pair electrons in the hard segments of WPUs, which results in a higher conductivity. In aliphatic WPU of PPG/IPDI, the dense arrangement of hard segments is reduced by the steric hindrance of IPDI cyclohexane in the *meta*-position. The lithium ions (on DMPA unit) are easily trapped into the phase of loose hard segments, leading to lower conductivity. In the PPG/H_{12}MDI aliphatic WPU, a dense arrangement of hard segments (relative to IPDI) is enhanced by the linear structure of H_{12}MDI. The lithium ions (on DMPA units) are difficult to pass through the polymer matrix.

The temperature dependence of conductivity with the addition of PC and external doping salt of 0.5 mmol/g WPU is shown in Fig. 7(b), revealing that the conductivity is highly increased. At this low concentration of salt, the ion transport in polymer electrolytes has a coupling of mobile charge carriers to the soft segmental motion of the polymer host. Because the soft segment domain belongs to PPG phase in all WPUs, the conductivity differences mainly arise from the hard segments. In aromatic WPUs, the arrangement of hard segments is closer due to stronger intermolecular/intramolecular H-bonding. Thus, the lithium ions mainly transport in the phase of soft segment, leading to a higher conductivity. In PPG/H_{12}MDI WPU, a close phase of hard segment is also obtained due to the linear symmetrical structure of H_{12}MDI, the lithium ions also transport in the phase of soft segment. In PPG/IPDI WPU, a loose phase of hard segment is obtained due to the low H-bonding and

unsymmetrical structure of IPDI. Thus, the lithium ions transport in both soft and hard segments. The concentration in the phase of soft segment is lowered, leading to a low conductivity.

As the concentration of external doping salt is further increased, the concentration of lithium ions is naturally increased. The effect of hard segment on the ionic conductivity becomes insignificant, resulting in similar conductivity for all types of WPUs as shown in Fig. 7(c) and (d).

4. Conclusions

The increase in the added salt of all WPU samples increases T_g. Except PPG/H_{12}MDI, the level of the added salt in other WPUs is saturated in the range of 0–2 mmol $LiClO_4$/g WPU. The phase separation of aromatic diisocyanate-based WPUs is more significant than that of aliphatic ones in the addition of salts. Without adding $LiClO_4$, WPU with the more significant phase separation possesses the lower conductivity as single-ion electrolytes. Meanwhile, the conductivity of WPU single-ion electrolyte for PPG/MDI is much more temperature sensitive than that for others. The conductivity of WPU based electrolytes increases or decreases with increasing the salt concentration as added salt level is unsaturated or saturated, respectively. In the addition of 2 mmol $LiClO_4$/g WPU and 50% PC, the effect of hard segment on the ionic conductivity becomes insignificant. In conclusion, phase separation/mixing due to different hard segments affects the conductivity of WPU electrolytes with/without the addition of salts and solvents.

Acknowledgements

The authors are grateful to the National Science Council in Taiwan for its financial support through NSC 88-2214-E-006-026.

References

[1] Armand MB, Chabagno JM, Dudot MJ. In: Vashista P, Mundy JN, Shenoy GK, editors. Fast ion transport in solids, Amsterdam: Elsevier/North-Holland, 1979. p. 131.
[2] Fenton DE, Parker DE, Wright PV. Polymer 1973;14:589.
[3] Gauthier M, Belanger A, Kapper B, Vassort G, Armand M. In: MacCallum JR, Vincent CA, editors. Polymer electrolytes: Review 2, London: Elsevier, 1989. p. 285.
[4] Przyluski J, Wieczorek W. Synth Met 1991;45:323.
[5] Cheng TT, Wen TC. J Electroanal Chem 1998;459:99.
[6] Cheng TT, Wen TC. Solid State Ionics 1998;107:161.
[7] Cheng TT, Wen TC. J Chin Inst Chem Engrs 1998;29:319.
[8] Wen TC, Wang YJ, Cheng TT, Yang CH. Polymer 1999;40:3979.
[9] Wen TC, Wu MS, Yang CH. Macromolecules 1999;32:2712.
[10] Van Bogart JV, Gibson PE, Cooper SL. J Polym Sci: Polym Phys Ed 1983;21:65.
[11] Yang CH, Lin SM, Wen TC. Polym Engng Sci 1995;35:722.
[12] Yang CH, Li YJ, Wen TC. I&EC 1997;36:1614.
[13] McLennaghan AW, Pethrick RA. Eur Polym J 1988;24:1063.
[14] McLennaghan AW, Hooper A, Pethrick RA. Eur Polym J 1989;25:1297.
[15] Watanabe M, Dohashi S, Sanui K, Ogata N, Kobayashi T, Ohtaki E. Macromolecules 1985;18:1945.
[16] Watanabe M, Sanui K, Ogata N. Macromolecules 1986;19:815.
[17] Schantz S, Torell LM, Stevens JR. J Chem Phys 1991;94:6862.
[18] Lee HS, Wang YK, Hsu SL. Macromolecules 1987;20:2089.
[19] Lu X, Weiss RA. Macromolecules 1991;24:4381.
[20] Lee SS, Wang YK, MacKnight WI, Hsu SL. Macromolecules 1988;21:270.
[21] Sung CSP, Schneider NS. Macromolecules 1977;10:452.
[22] Pollack SK, Shen DY, Hsu SL, Wang Q, Stidham HD. Macromolecules 1989;22:551.
[23] Van Heumen JD, Stevens JR. Macromolecules 1995;28:4268.
[24] Schantz S, Torell LM, Stevens JR. J Chem Phys 1991;94:6862.